



Cite this: *Environ. Sci.: Nano*, 2025, 12, 1177

## UV-B degradation affects nanoplastic toxicity and leads to release of small toxic substances†

Mikael T. Ekvall,<sup>‡,ab</sup> Raluca Svensson,<sup>a</sup> Josep García Martínez,<sup>id c</sup> Annette M. Krais,<sup>c</sup> Katja Bernfur,<sup>a</sup> Thom Leiding,<sup>a</sup> Martin Lundqvist <sup>id ‡,ab</sup> and Tommy Cedervall <sup>id \*ab</sup>

Fragmented micro- and nanoplastics are widespread pollutants with adverse effects on the environment. However, the breakdown process does not end with micro- and nanoplastics but is expected to continue until carbon dioxide has been formed. During this process the plastics will undergo chemical changes and small molecules may be released. We have broken down small amine-modified (∅53 nm) and carboxyl-modified (∅62 nm) polystyrene nanoparticles by UV-B irradiation during 100 days. We see a decreasing size and an oxidation of the nanoparticles over time. Simultaneously, the acute toxicity to zooplankton *Daphnia magna* decreases. UV-B irradiation releases small, dissolved molecules that are toxic to *Daphnia magna*. The dissolved molecules include aminated alkyls, styrene remnants and secondary circularization products. The study shows that UV-B radiation can change the original toxicity of nanoplastics and release new toxic substances.

Received 30th August 2024,  
Accepted 11th December 2024

DOI: 10.1039/d4en00795f

rsc.li/es-nano

### Environmental significance

Our understanding of the effect of ultraviolet radiation (UV) on the breakdown of nanoplastic in nature is negligible. While the effects on larger plastics have been studied, there is, to our knowledge, a current gap when it comes to nanoplastic (<100 nm) breakdown and how this UV mediated breakdown may affect the material and the potential toxicity of the material. We show how UV exposure affects polystyrene nanoparticles, resulting in particle breakdown and a reduced toxicity of an amine-modified particle that is toxic towards the freshwater zooplankter *Daphnia magna* in its pristine form. We also show that a complex toxic mixture of small molecules is released during the breakdown process. This study highlights potential outcomes of UV mediated nanoplastic breakdown.

## Introduction

Micro- and nanoplastic particles are currently ubiquitous and present in all compartments of the natural environment where they can be retained and taken up by organisms and induce ecotoxicological issues, both by the direct toxicological effect at the species level and through cascading effects.<sup>1–3</sup> Nanoplastics are defined as plastic pieces that have been degraded in nature to a size below 100 nm<sup>4</sup> or 1 μm.<sup>5</sup> Nanoplastics are, due to their small size, difficult to isolate in nature but were first found in the Atlantic in 2017.<sup>6</sup> Studies confirm the abundance of nanoplastics and suggest there is up to 0.5 mg L<sup>-1</sup> nanoplastics in Swedish lakes close to cities.<sup>7</sup> The size distribution between

micro- and nanoplastics has recently been measured in mussels with an interesting result that the mass (187 ng mg<sup>-1</sup>) of the nanoplastic fraction (20–200 nm) is similar to the mass (216 ng mg<sup>-1</sup>) of the microplastic fraction (≥2.2 μm).<sup>8</sup> In a comparison based on the particle number or surface area, nanoplastics will dominate and may therefore have a greater impact on biological effects. For example, small carboxylated polystyrene nanoparticles inhibit plasma coagulation by binding to the active site in Factor XIIIa in the coagulation cascade, whereas larger particles activate coagulation by providing a surface for the activation complex.<sup>9</sup>

Polystyrene is the 6th most consumed plastic,<sup>10</sup> but none or only small amounts of polystyrene nanoplastics were found in Swedish lakes.<sup>7</sup> However, in mussels, the ratio followed the expected pattern for polystyrene nanoplastics.<sup>8</sup> Polystyrene nanoplastics have also been found in soil.<sup>11</sup> The release of polystyrene nanoplastics after ultraviolet (UV) irradiation of polystyrene coffee cup lids was shown in 2016,<sup>12</sup> and from plastic sheets and boxes in 2023.<sup>13,14</sup> The release of micro- and nanoplastics from commercial micro-sized polystyrene beads after UV irradiation has been demonstrated.<sup>15,16</sup> Furthermore,

<sup>a</sup> Biochemistry and Structural Biology, Lund University, P.O. Box 124, SE-221 00, Lund, Sweden. E-mail: tommy.cedervall@biochemistry.lu.se

<sup>b</sup> NanoLund, Lund University, P.O. Box 118, SE-221 00, Lund, Sweden

<sup>c</sup> Centre for Analysis and Synthesis (CAS), Lund University, Lund, Sweden

† Electronic supplementary information (ESI) available. See DOI: <https://doi.org/10.1039/d4en00795f>

‡ Equal contribution.



the release of nanoplastics from expanded polystyrene foam and coffee cup lids after being subjected to mechanical force was shown in 2019<sup>17</sup> and, in 2021, from expanded polystyrene after mild mechanical forces mimicking the mechanical friction in the ocean.<sup>18</sup> The nanoplastics formed from the mechanical degradation were chemically transformed, as compared to the starting material, and a higher level of oxygen was found in the formed nanoparticles.<sup>17,18</sup> Furthermore, styrene oligomers have been detected worldwide in sand and seawater at mean concentrations of  $3679 \pm 8199.2 \text{ ng g}^{-1}$  and  $5.1 \pm 6.4 \text{ ng L}^{-1}$ , respectively.<sup>19</sup> In the Pacific Ocean, the mean concentration of styrene oligomers has been measured to be  $1.48 \mu\text{g L}^{-1}$  and  $1.32 \mu\text{g L}^{-1}$  in surface water and deep water, respectively.<sup>20</sup> The styrene oligomers are expected to originate from polystyrene indicating that the presence of styrene oligomers is a result of the degradation occurring in nature.

Many possible intermediate breakdown products can originate from polystyrene subjected to UV irradiation during the degradation process, but continued UV irradiation ultimately results in carbon dioxide.<sup>21</sup> The mechanisms behind UV mediated degradation of polystyrene have been studied for decades and are reviewed by, for example, Yousif and Haddad, 2013,<sup>22</sup> and later from a micro-/nanoplastics in the environment perspective by Andrady, *et al.*, 2022.<sup>23</sup> High intensity UV irradiation of carboxyl-modified polystyrene beads, 0.1 to 2.5  $\mu\text{m}$ , continued the degradation processes until the polystyrene was totally broken down to mostly carbon dioxide and other volatile compounds.<sup>24</sup> Volatile compounds such as benzene, toluene, styrene and phenol have been detected after UV irradiation.<sup>25</sup> In addition, cyclization products were found after long-term irradiation of polystyrene films.<sup>26</sup> Different additives and stabilizers will also affect the resulting degradation products.<sup>21,22</sup> In conclusion, it seems likely that there is a complex mixture of various compounds released during the UV-mediated degradation of polystyrene.

An interesting aspect of micro- and especially nanoplastics is that the penetration depth of UV radiation is much larger than the particle diameter,<sup>27</sup> which also affects the energy absorption of the polystyrene. An effect of this may have been seen in the degradation of carboxyl-modified polystyrene microbeads as they were reported to start to degrade from the inside first and the decrease in diameter of the particles came later in the degradation process,<sup>24</sup> whereas other studies have only reported a shrinking diameter,<sup>15,28</sup> suggesting that the particles are degraded from the outside. The detection of only surface oxidation following short-term irradiation of radiolabeled 230 nm polystyrene nanoparticles indicates that surface degradation is occurring.<sup>29</sup> Higher UV intensity, longer irradiation time, and smaller size of the microbeads accelerated the release of dissolved organic matter.<sup>28</sup> The contents in the media, as *e.g.*, dissolved organic matter,<sup>30</sup> also affect the UV mediated degradation. The impact of UV irradiation on microplastic behaviour and effects on the environment has been reviewed (see *e.g.*, Cheng *et al.*, 2021<sup>31</sup>), and include effects on migration, release of additives, interactions with pollutants, and toxicity.

Although there is a rapidly growing number of articles describing the UV mediated degradation of microplastics, particles with an original size smaller than 100 nm have, to our knowledge, not been studied. Furthermore, the link between toxicity and UV mediated degradation needs to be examined in more detail to predict potential environmental effects related to the degradation process. Small, positively charged, amine-modified polystyrene nanoparticles are a good starting material to study. These particles have previously been shown to be acutely toxic to the freshwater zooplankton *Daphnia magna*.<sup>32</sup> However, in the same study it was shown that larger polystyrene particles, with similar or different surface modifications, were not acutely toxic.<sup>32</sup> Similar results were shown for amine-modified polystyrene nanoparticles ranging between 20 and 100 nm, where all particles were toxic but 20 and 40 nm exhibited stronger toxicity.<sup>33,34</sup> A size dependent toxicity seems to be a general feature among plastic nanoparticles as reviewed by Pikuda *et al.*, 2023.<sup>35</sup> We have studied here the physical degradation of 53 nm amine-modified polystyrene nanoparticles and compared the degradation with 62 nm carboxyl-modified polystyrene nanoparticles. We have further followed the acute toxicity, which was shown to decrease for the 53 nm particles after UV irradiation. However, a dissolved fraction from the degradation products was shown to be toxic to *D. magna*.

## Materials and methods

### Model particles and UV-B lamp

Two different polystyrene particles were bought from Bangs Laboratories Inc., USA. Particle 1 had a mean diameter of 53 nm and an amine-modified surface (catalogue code: PA02N, lot nr.: 15045). Particle 2 had a mean diameter of 62 nm and carboxyl-modified surface (catalogue code: PC02N, lot nr.: 11652). Both particles were delivered in a colloidal suspension with a concentration of  $\approx 10\%$  solids (w/w) according to the manufacturer.

To remove the additives, the particle solution was transferred to a dialyzed tube, (MilliPore MWCO 3000), and thoroughly dialyzed against MilliQ H<sub>2</sub>O before further use.

UV-B lamps, ExoTerra Reptile UV-B 200, 25 W, were purchased from a local pet shop. The lamps emitted wavelength spectra, taken with an air-coupled Avantes Czerny-Turner mini spectrometer with 2048 pixels and a 10  $\mu\text{m}$  slit with a 1 ms integration time, which can be found in Fig. S1.†

### UV-B treatment of particles

The dialyzed 53 nm amine-modified particles were diluted 40 $\times$  with MilliQ H<sub>2</sub>O to a final concentration of  $\approx 0.25\%$  (w/w) or  $\approx 2.5 \text{ mg mL}^{-1}$ . 80 ml of the solution was transferred to Petri dishes, either made of quartz or glass, and placed in a fridge. Three UV-B lamps were fitted in a cardboard box to shield the surrounding environment from UV radiation, as shown in Fig. S2,† so the lamps tips were 10 cm over the Petri dishes. When the three lamps were turned on, the



temperature in the cardboard box, inside the fridge on maximum cooling, was stable at  $21 \pm 1$  °C.

The 62 nm carboxyl-modified particles were treated the same way except that they were diluted 2000× with MilliQ H<sub>2</sub>O to a final concentration of  $\approx 0.005\%$  (w/w) or  $\approx 0.05$  mg mL<sup>-1</sup>.

The quartz Petri dish was chosen since the material allows for wavelengths in the UV range to pass through the material while the glass Petri dish was chosen as a control since it was expected to filter out the UV wavelengths.

### DLS measurements

The size distribution of the 53 nm amine-modified and 62 nm carboxyl-modified samples were analysed using a DynaPro Plate Reader II from Wyatt Technology, USA. Measurements were carried out in 96-well half width plates manufactured by Corning. Four 100 μL sub-samples of each treatment (UV-B exposed and un-exposed, respectively) were loaded into separate wells. The measured value from each well is based on 10 consecutive measurements at 25 °C.

### DSC measurements

After the end of the exposure period the particles were diluted five times in MilliQ H<sub>2</sub>O and 100 μL of each sample was applied to an 8–24% sucrose gradient capped with 0.5 mL of dodecane and analysed at 24 000 rpm on a DC24000 disc centrifuge (CPS Instruments, USA).

### Zeta potential measurements

The zeta potentials were determined using a Zetasizer Ultra, Mavern Analytical, United Kingdom. The software used was ZS XPLOER 2.0.1.1. Cuvettes, DTS1070, from Malvern Analytical were used for all measurements. Each sample was measured three times with at least 30 runs for each measurement and the temperature was set to 25 °C. The analysis model was set to auto.

### FTIR measurements

A Spectrum Two FTIR equipped with a UATR Two unit from PerkinElmer was used to record the FTIR spectra. 6–10 μL of the sample was placed on the crystal of the UATR unit, and H<sub>2</sub>O was allowed to evaporate for 30–45 minutes before the spectrum was recorded. This process does not always work due to how the particles migrate during the drying, as shown in Fig. S8.† The spectrum was processed using the PerkinElmer Spectrum IR application, version 10.7.2.1630. The data presented in this article has been corrected using Data Tune-up and Interactive Baseline Correction.

### Acute toxicity tests

An acute toxicity test on the UV-B exposed and UV-B shaded particle dispersions (*i.e.* 53 nm and 62 nm, see above) was performed using the freshwater zooplankton *D. magna*. One neonate was put in a 50 mL Falcon tube containing 40 mL of

either the UV-B exposed or UV-B shaded particle dispersed in tap water with a nanoplastic concentration of 5 mg L<sup>-1</sup>. A control treatment containing tap water only was prepared and ran alongside the particle exposures as a reference. Each treatment was replicated 15 times and all experimental groups were kept at 18 °C temperature with 16:8 hours light/dark cycle. The experiment lasted for 48 hours, and the *D. magna* were not fed during the experiment.

### Particle separation and acute toxicity tests

The 53 nm particles were separated from small molecules by applying 250 μL on a PD10 column (Cytoviva). An additional 750 μL H<sub>2</sub>O was added before the samples were eluted in 1 mL steps with H<sub>2</sub>O. Each fraction was analysed by measuring the absorbance at 230 nm. Fractions 3 to 5 containing the particles or particle remnants, and fractions 8–9 containing the smaller breakdown molecules were pooled. For the toxicity tests on *D. magna* 12 separations were made and pooled. The toxicity tests were carried out in 10 replicates in a total volume of 9 mL of which the collected fractions were 1.5 mL and 7.5 mL ISO test water or 1.5 mL Milli-Q water and 7.5 mL ISO test water in the controls testing the 53 nm particle. The ISO test water used was prepared according to OECD 202 test guidelines.<sup>36</sup> The particle concentration was approximately 50 mg L<sup>-1</sup>. The survival was checked regularly for 24 hours.

### Detection of small molecules

Fractions 10–11 from the separation were analysed by mass spectrometry (MS). MS spectra were acquired using an Autoflex Speed MALDI TOF/TOF mass spectrometer (Bruker Daltonics, Bremen, Germany) in the positive reflector mode. The sample was acidified to a concentration of 0.5% trifluoroacetic acid (TFA) before a 1 μL sample was mixed with 0.5 μL Matrix solution, consisting of 5 mg mL<sup>-1</sup> α-cyano-4-hydroxy cinnamic acid, 80% acetonitrile, and 0.1% TFA, and added to a MALDI stainless steel plate. The spectrum was externally calibrated using peptide calibration standard II (Bruker Daltonics) containing 9 internal standard peptides.

The fractions 10–11 were subjected to non-targeted analysis using an Agilent HPLC 1290 equipped with a Acquity HSS C18 column (3.0 × 100 mm, 1.8 μm), connected to a Bruker timsTOF Pro 2 *via* a 6-port valve, which allowed to inject a calibration solution in each injection and recalibrate mass and mobility for more accurate results. The calibration solution used was a mixture of Agilent ESI-Low concentration Mix for mobility and sodium formate for mass calibration. The calibration segment was 0.5 min and the total analysis time was 18 min. Acetonitrile (0.1% formic acid) and water (0.1% formic acid) were used as the mobile phase with a flow of 0.4 mL min<sup>-1</sup>. The range of *m/z* was 20–1300, and the range of mobility was set according to that range to find small molecules. The sample was analysed in the positive and negative mode together with an instrument blank, each in triplicates. The data obtained was later processed with



Metaboscope (2022b) and using the NORMAN target list<sup>37</sup> to tentatively identify compounds. Thereafter, the data was further processed by an in-house R script to filter out false positives by using the repetitions and blanks. InChIKeys were used to predict mobility and MS/MS fragmentation. If the prediction was not good enough (>5% for mobility), the features were deleted.

### Statistical analysis

Size differences between UV-B exposed and unexposed materials were evaluated using *t*-tests. *D. magna* survival in acute toxicity tests was evaluated using Kaplan–Meier survival analysis and the *p*-value was attained from the log-rank (Mantel-Cox) test. All statistical evaluations were performed using GraphPad Prism (version 8.4.3).

## Results and discussion

### UV-B exposure of 53 nm amine-modified polystyrene particles – size

The overall aim of this study was to investigate if UV radiation affects the acute toxicity to *D. magna* exhibited by small, positively charged, amine-modified polystyrene nanoparticles. Two characteristics of these particles, their small size and positive charge, are thought to confer the toxicity. Both these characteristics can possibly be changed by UV-B exposure. Therefore, we exposed 53 nm amine-modified polystyrene particles to UV-B radiation in a controlled laboratory setup, as shown in Fig. S2.† After 100 days of UV-B exposure, optical examination revealed striking differences between the sample and the control as the 53 nm particle dispersion has changed colour from white to brownish and from opaque to clear, compared to the UV-B shaded control, as shown in Fig. S3 and S4.† The particle size was characterized using DLS after the UV-B exposure. The DLS measurements show that UV-B exposure significantly decreases the size of the particles compared to unexposed particles ( $t = 4.796$ ,  $df = 6$ ,  $p = 0.003$ ), as shown in Fig. 1 and

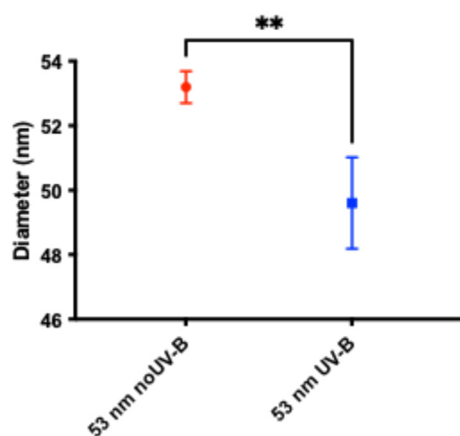


Fig. 1 The size difference measured by DLS after 100 days UV-B exposure showing that the particle size significantly decreased after UV-B treatment compared to the control.

Table 1 Size and zeta potential of the particles

| Method        | DLS <sup>a</sup> | Zeta potential <sup>b</sup> |
|---------------|------------------|-----------------------------|
|               | Size (nm)        | (mV)                        |
| Control 53 nm | 53.2 ± 0.5       | 27.8 ± 1.3                  |
| UV-B 53 nm    | 49.6 ± 1.4       | 28.8 ± 0.6                  |

<sup>a</sup> DynaPro. <sup>b</sup> Zetasizer Ultra.

Table 1. A decreasing size of micro-sized polystyrene particles after high intensity UV exposure has been demonstrated before.<sup>15</sup> The results confirm that in low intensity UV-B exposure the same processes can be seen, however, the time scale is much longer.

The size of the particles was further characterized with DSC, which, in contrast to DLS, shows that UV-B exposure increases the particle size and broadens the size distribution, as shown in Fig. 2. The techniques differ, as DLS calculates the particle size based on Brownian motions and DSC from the sedimentation time through a sucrose gradient. Therefore, a possible interpretation of the contrasting results is that UV-B irradiation breaks up the polystyrene chain resulting in less compressed particles or particles with less material due to partial degradation in the entire particle.<sup>24</sup> Both cases would facilitate the exchange of water to sucrose in the internal of the particles, resulting in a higher density of the newly formed particles which could explain the observed results.

### UV-B exposure of 53 nm amine-modified polystyrene particles – chemistry

As mentioned above, a possible explanation for the acute toxicity exhibited by the small amine-modified polystyrene particles is their positive surface charge. However, the zeta potential did not significantly change after 100 days of UV-B

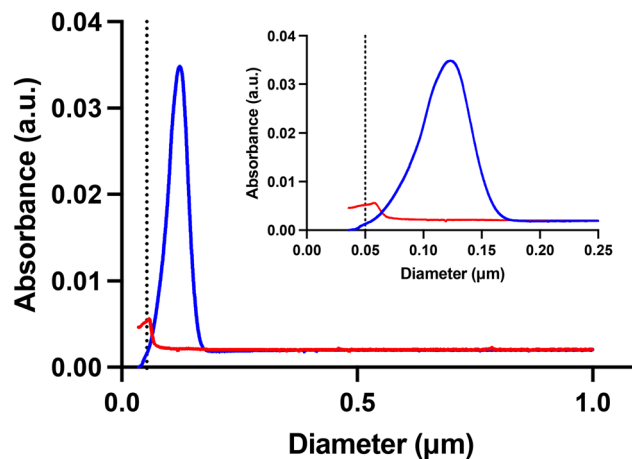


Fig. 2 The size difference measured by DSC after 100 days UV-B exposure. UV-B treated particles are in blue and untreated in red. The dotted vertical line indicates the nominal size of the starting material, i.e. 53 nm. The inset plot shows a zoom of the size range of 0–250 nm.



exposure (Table 1, Fig. S5†). These results could lead to various interpretations, such as the possibility that most amine groups remain intact or that the chemical changes still resulted in positively charged surface groups. However, as thoroughly reviewed by S. Bhattacharjee, measuring the zeta potential of nanoparticles reveals very little about the actual surface charge of the nanoparticles.<sup>38</sup>

The UATR-FTIR spectra for the control (red) and UV-B-treated (blue) samples are shown in Fig. 3. Four grey arrows indicate regions in the spectra exhibiting differences. Three of these, arrows 1, 2 and 4, are associated with oxygen bounds. The carbonyl index is used to measure the chemical oxidation of polymers. Almond *et al.* extensively reviewed various methods for calculating the carbonyl index (CI); in their article, they recommended the use of the specified area under band (SAUB) methodology.<sup>39</sup> The CIs were computed using the formula  $CI = \text{area under band } 1850\text{--}1650 \text{ cm}^{-1} / \text{area under band } 1500\text{--}1420 \text{ cm}^{-1}$ . The carbonyl index (CI) values, as shown in Fig. S6,† further underscore the distinction between the control (CI  $\approx$  1.0) and UV-B treated (CI  $\approx$  2.0) samples.

Arrow 3 indicates the absorbance peak at  $1602 \text{ cm}^{-1}$ , which is indicative of conjugated C=C systems. A closer inspection of the signal reveals that the absorbance at  $1602 \text{ cm}^{-1}$  increases compared to the C-H regions,  $3100\text{--}2840$  and  $1500\text{--}1440 \text{ cm}^{-1}$ . Hence, the chemistry of the polystyrene nanoparticles is altered by the UV-B irradiation.

#### UV-B exposure of 53 nm amine-modified polystyrene particles – toxicity

The untreated 53 nm amine-modified polystyrene particles were, as expected, toxic to *D. magna*, ( $\chi^2_{(df=1)} = 24.18$ ,  $p < 0.0001$ ), as shown in Fig. 4, which has been reported before.<sup>32</sup> The UV-B exposed sample was still toxic to *D. magna*, ( $\chi^2_{(df=1)}$

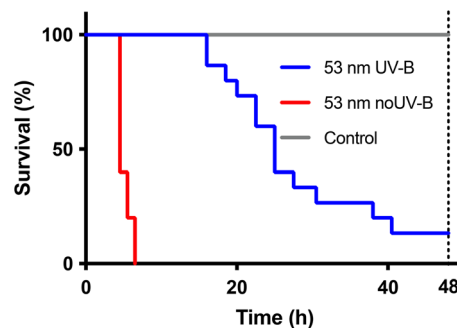


Fig. 4 Acute toxicity test with 53 nm amine-modified polystyrene particles. Kaplan-Meier survival curves for *D. magna* exposed to UV-B exposed (blue line) and UV-B shaded (red line) nanoplastics. The grey line shows a control treatment only containing water. Total exposure time is 48 hours as highlighted by the dotted vertical line.

$= 32.81$ ,  $p < 0.0001$ ) compared to the control. However, the toxicity was significantly reduced ( $\chi^2_{(df=1)} = 32.81$ ,  $p < 0.0001$ ) compared to the untreated particles. It is likely that the oxidation by UV-B exposure have changed the particles to more resemble polystyrene and oxidized polystyrene than the starting material amine-modified polystyrene. This could explain the decreased toxicity as neither plain nor carboxyl-modified polystyrene nanoparticles are acutely toxic.<sup>32</sup>

#### UV-B exposure of 53 nm amine-modified polystyrene particles – dissolved fraction

It has been reported that intense UV irradiation of polystyrene results in the release of many different small dissolved organic compounds into the media.<sup>25,26,40</sup> We therefore expect that UV-B exposure also can result in the release of small molecules. To further analyse the samples, the small, dissolved molecules were separated from particles by applying the UV-B exposed mixture to a PD10 column. The 53 nm particles elute in fractions 3–5, and the small, dissolved molecules elute in fractions 10–11, as shown in Fig. 5A. The total amount of carbon and nitrogen was determined using a Shimadzu TOC-V CPH equipped with a nitrogen detector, before and after separation, as shown in Table 2. The carbon/nitrogen ratio is higher for the particle fractions but lower for the dissolved molecules after separation, which is consistent with the observation that nitrogen disappears from the surface of the particles.

The separated samples were tested for toxicity with an acute toxicity test, as shown in Fig. 5. Interestingly, the fractions containing the dissolved molecules produced from the UV-B exposure exhibited a significant toxicity compared to the control ( $\chi^2_{(df=1)} = 19.41$ ,  $p < 0.0001$ ). In agreement with the first experiment, Fig. 4, the UV-B exposed particles are less toxic than the untreated particles ( $\chi^2_{(df=1)} = 16.35$ ,  $p < 0.0001$ ). The time when immobilization occurs and the resolution between the samples are different; this could be due to several reasons. As we aimed for a higher concentration of dissolved breakdown molecules, the concentration here is 10× higher as compared to

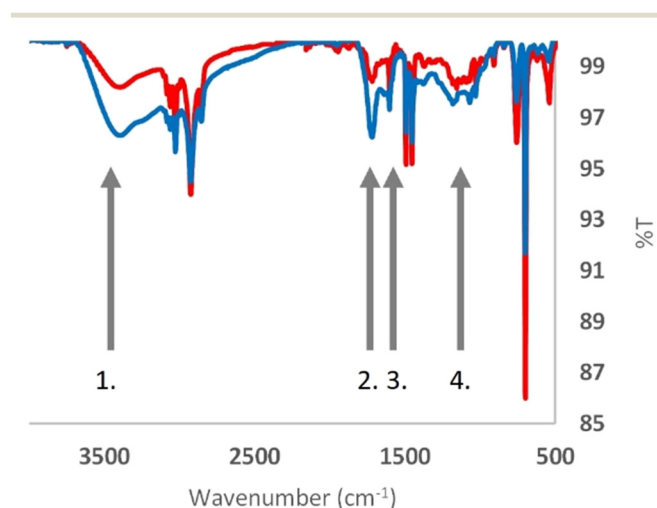


Fig. 3 UATR-FTIR spectra for the 53 nm PS-NH<sub>2</sub> particles. Red is the control, placed in a glass Petri dish during the experiment, sample. Blue is the UV-B treated, placed in a quartz Petri dish during the experiment, sample. The grey arrows indicate some of the changes in the FTIR spectra.





**Fig. 5** The acute toxicity of the separated samples after passing the PD10 column. The separation of untreated and treated articles by a PD10 column (A). The inset zooms in at the pooled fractions 10–11. The acute toxicity of the different fractions (B). In red is the pooled fractions 3 to 5 of the UV-B shaded sample. In blue is the pooled fractions 3 to 5 of the UV-B exposed sample. In orange is the pooled fractions 10 to 11 of the UV-B exposed sample. In black is the control sample (no particle fraction added).

**Table 2** Carbon and nitrogen content in the fractions after separation

| Sample                   | Carbon<br>(mg L <sup>-1</sup> ) | Nitrogen<br>(mg L <sup>-1</sup> ) | Carbon/nitrogen |
|--------------------------|---------------------------------|-----------------------------------|-----------------|
| Unseparated              | 2614                            | 32.9                              | 79.5            |
| NP fraction <sup>a</sup> | 257                             | 2.0                               | 128.5           |
| DM fraction <sup>a</sup> | 21.4                            | 1.3                               | 16.5            |

<sup>a</sup> Diluted 8–10 times compared to the unseparated fraction.

the previous test. The experimental design, with a smaller volume compared to the other assay, was limited by the sample volume and aimed at determining if the dissolved compounds are toxic.

The dissolved small molecules were analysed by mass spectrometry, as shown in Fig. S7.† Notably in the spectra is a 44-mass unit repeat. This could be an oxidized two carbon unit as C<sub>2</sub>OH<sub>4</sub> that has a molecular mass of 44. The smallest weight we can detect is 626, which would mean a chain with 28 carbons.

The dissolved fraction was further described with untargeted analysis. The detected compounds are shown in Table 3 and with the structure in Table S1.† It is evident that the UV-B exposure results in a very complex mixture of dissolved compounds, including molecules containing nitrogen. There

are examples of molecules indicating ring opening resulting in long carbon chains. There are oxidized carbon chains, which support the results from the mass spectrometry data described above. In four molecules the nitrogen is within a closed ring indicating complexed secondary cyclization reactions, which have been described before.<sup>26</sup> Sulphone groups are present, which is probably from the original polystyrene nanoparticles that are aminated. We have previously shown that aminated polystyrene nanoparticles have a batch dependent FTIR signal, probably due to the level of amination.<sup>41</sup> Three molecules, amine alkyls, 12-aminododecanoic acid, and 4-methyl-2-pentylpyridine, are labelled with health/environmental hazards. Nine of the identified molecules can be described as amine detergents. The evaluation of the toxicity of 20 amine detergents to *D. magna* showed that alkyl chains with a single nitrogen at the end were more toxic than oxidized amine alkyls.<sup>42</sup> The found amine alkyls may therefore contribute more to the toxicity than the 8 oxidized amine detergents. Prolonged UV irradiation should induce more oxidation and thereby with time decrease the toxicity. Furthermore, the production of amine detergents could affect the physical behaviour and toxicity of the remaining polystyrene nanoparticles.<sup>43</sup> However, many of the other identified molecules may contribute to the toxicity but, to our knowledge, are not tested.

## 62 nm carboxyl-modified polystyrene nanoparticles

We wanted to further explore the UV-B efficiency in breaking down polystyrene and to see if the process could generate small toxic molecules from a nanoparticle that is not acutely toxic for *D. magna*. The choice fell upon the 62 nm carboxyl-modified polystyrene nanoparticles. In contrast to the 53 nm amine-modified polystyrene nanoparticles, the 62 nm carboxyl-modified polystyrene nanoparticles exhibit no acute toxicity.<sup>32</sup>

The size of the carboxyl-modified nanoparticles during degradation was followed using DLS, as shown in Fig. 6. The effect of the UV-B radiation is slow during the first 20 days; after that, it accelerates, and DLS cannot detect any particles in the treated sample after 79 days of treatment. The degradation of the 62 nm particles is significantly faster than the degradation of the 53 nm particles. A plausible explanation for this is the lower concentration, 50× less, of the particle dispersion in the 62 nm experiment, which means that the light will hit each particle in the sample more often. Another difference between the two UV-B experiments is that new UV lamps were used in the 62 nm carboxyl-modified polystyrene particle experiment. Based on our later lamp characterization, as shown in Fig. S1,† it is clear that the lamp age affects the spectral intensity of the lamp. The combination of lower particle concentration and new UV-B lamps could explain the faster photo-degradation observed in the 62 nm carboxyl-modified polystyrene particle experiment, as shown in Fig. 6.

The degradation process of the 62 nm carboxyl-modified polystyrene particles was followed by UATR-FTIR. Fig. S8†



**Table 3** Non-targeted analysis of the compounds in the dissolved fractions 10–11. After UV-B breakdown of the aminated polystyrene nanoparticles the dissolved molecules were separated from the remaining particles and analysed for the contents

|    | Name   | Molecular formula   | Hazard             |
|----|--|---|--------------------|
| 1  | (2-Neopentylallyl)succinic acid                                  | C <sub>12</sub> H <sub>20</sub> O <sub>4</sub>                  |                    |
| 2  | (2Z,4S,5S,6S,7R,8Z)-2,9-Diphenyldeca-2,8-diene-3,4,5,6,7,8-hexol | C <sub>22</sub> H <sub>26</sub> O <sub>6</sub>                  |                    |
| 3  | (5-Ethyl-2,2-dimethyl-1,3-dioxan-5-yl)methyl acrylate            | C <sub>12</sub> H <sub>20</sub> O <sub>4</sub>                  |                    |
| 4  | 3-(hexadecyloxy)-1-propanamine                                   | C <sub>19</sub> H <sub>41</sub> NO                              |                    |
| 5  | 12-(Methylamino)dodecanoic acid                                  | C <sub>13</sub> H <sub>27</sub> NO <sub>2</sub>                 |                    |
| 6  | 12-Aminododecanoic acid  | C <sub>12</sub> H <sub>25</sub> NO <sub>2</sub>                 | Health             |
| 7  | 2-Hydroxypropyl hexanoate  | C <sub>9</sub> H <sub>18</sub> O <sub>3</sub>                   |                    |
| 8  | 3-(Hexadecylamino)propane-1,2-diol                               | C <sub>19</sub> H <sub>41</sub> NO <sub>2</sub>                 |                    |
| 9  | 3-Ethylaniline   | C <sub>8</sub> H <sub>11</sub> N                                |                    |
| 10 | 3-[(Acetoxy)methyl]nonan-1-oic acid                              | C <sub>12</sub> H <sub>22</sub> O <sub>4</sub>                  |                    |
| 11 | 4-Methyl-2-pentylpyridine  | C <sub>11</sub> H <sub>17</sub> N                               | Environment        |
| 12 | 5-Amino-1,1-dimethylhexyl acetate                                | C <sub>10</sub> H <sub>21</sub> NO <sub>2</sub>                 |                    |
| 13 | 5-Butyl-2-methylpyridine   | C <sub>10</sub> H <sub>15</sub> N                               |                    |
| 14 | A-[(2-Methylpropoxy)methyl]pyrrolidine-1-ethanol                 | C <sub>11</sub> H <sub>23</sub> NO <sub>2</sub>                 |                    |
| 15 | A-Hydroxy- <i>p</i> -methoxytoluene- <i>a</i> -sulphonic acid    | C <sub>8</sub> H <sub>10</sub> O <sub>5</sub> S                 |                    |
| 16 | Amines, C16–22-alkyl   | C <sub>19</sub> H <sub>41</sub> N                               | Health/environment |
| 17 | C13 alkyl dimethyl betaine                                       | C <sub>17</sub> H <sub>35</sub> NO <sub>2</sub>                 |                    |
| 18 | C15 alkyl dimethyl betaine                                       | C <sub>19</sub> H <sub>39</sub> NO <sub>2</sub>                 |                    |
| 19 | C17 alkyl dimethyl amine oxide                                   | C <sub>19</sub> H <sub>41</sub> NO <sub>2</sub>                 |                    |
| 20 | Calcium bis(hydroxybenzenesulphonate)                            | C <sub>12</sub> H <sub>10</sub> CaO <sub>8</sub> S <sub>2</sub> |                    |
| 21 | Cyclohexylmethyl-2,3-dihydroxy-5-methyl-hexylamide               | C <sub>14</sub> H <sub>29</sub> NO <sub>2</sub>                 |                    |
| 22 | Dodec-2-enedioic acid  | C <sub>12</sub> H <sub>20</sub> O <sub>4</sub>                  |                    |
| 23 | Piperidine-1,2-diethanol   | C <sub>9</sub> H <sub>19</sub> NO <sub>2</sub>                  |                    |
| 24 | TRADECAMIDE  | C <sub>15</sub> H <sub>31</sub> NO <sub>2</sub>                 |                    |

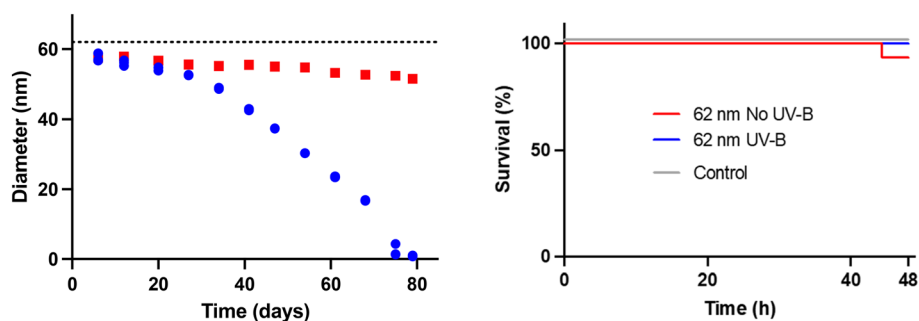


**Fig. 6** UV-B exposure of 62 nm carboxyl-modified polystyrene particles. Left. Particle size was followed by DLS. The UV-B treated samples are shown in blue, and the UV-B shaded samples are shown in red. The dotted horizontal line represents the nominal size of the particles as stated by the manufacturer (i.e. 62 nm). Right. Acute toxicity test with 62 nm carboxyl-modified polystyrene particles. Kaplan–Meier survival curves for *D. magna* exposed to UV-B exposed (blue line) and UV-B shaded (red line) nanoplastics. Grey line shows a control treatment only containing water. Each treatment was replicated 15 times, and the exposure concentration is 5 mg L<sup>-1</sup>. No significant differences were identified,  $p > 0.05$ .

shows the spectra from five different time points and Fig. S6† shows the calculated CI. Compared to the CI for the amine-modified particles, the CI is higher for the carboxyl-modified particles and is decreasing for the first two time points after which it fluctuates. In the later time points (data not shown) the data is difficult to collect.

The samples were too diluted to give a reliable determination of the zeta potential.

#### Toxicity test with 62 nm carboxyl-modified polystyrene nanoparticles and its breakdown products

As shown previously, the degradation products from the amine-modified particles caused acute toxicity. In light of this, we

wanted to investigate if the degradation products from a normally benign particle, the 62 nm carboxyl-modified polystyrene particle, would be acutely toxic to *D. magna*. After 79 days of UV-B exposure, there were no detectable particles, indicating complete or near complete particle degradation, hence the sample only contains degradation products. This sample was tested for toxicity to *D. magna*, as shown in Fig. 6. As expected, no toxicity was observed for the untreated particles ( $p > 0.05$ ) although the concentration of particles was the same as for the amine-modified polystyrene nanoparticles. Likewise, there was no toxicity observed for the UV-B treated sample either ( $p > 0.05$ ). Although the concentration of dissolved compounds is unknown, the potential concentration is probably higher for the dissolved fraction originating from the carboxyl-



modified polystyrene particles than that from the amine-modified polystyrene particles, since only a small fraction of the amine-modified particles was degraded. This may suggest that the degradation products from the amine-modified polystyrene are much more toxic. However, since the degradation process was faster for the 62 nm carboxyl-modified polystyrene particles, due to lower particle concentration and new lamps, there is a possibility that we missed a point on the degradation road that would be toxic, but the compounds have either evaporated or degraded further before we started the toxicity test. The answer to this question is beyond the scope of this article.

## Conclusions

- UV-B exposure decreases the size of 53 nm amine-modified and 62 nm carboxyl-modified polystyrene particles.
- The toxicity to *D. magna* decreases after UV-B exposure of the 53 nm amine-modified polystyrene particles.
- UV-B degradation releases a complex mixture of small molecules that are toxic when originating from the 53 nm amine-modified nanoparticles.
- UV-B degradation of the 62 nm carboxyl-modified nanoparticles did not result in any, for *D. magna*, acutely toxic compound.

## Data availability

The data supporting this article will be included as part of the ESI.†

## Conflicts of interest

There are no conflicts to declare.

## References

- 1 B. R. Kiran, H. Kopperi and S. V. Mohan, Micro/nanoplastics occurrence, identification, risk analysis and mitigation: challenges and perspectives, *Rev. Environ. Sci. Bio/Technol.*, 2022, **21**, 169–203.
- 2 F. Ståbile, M. T. Ekvall, J. A. Gallego-Urrea, T. Nwachukwu, W. G. C. U. Soorasena, P. I. Rivas-Comerlati and L.-A. Hansson, Fate and biological uptake of polystyrene nanoparticles in freshwater wetland ecosystems, *Environ. Sci.: Nano*, 2024, **11**, 3475–3486.
- 3 M. T. Ekvall, F. Ståbile and L.-A. Hansson, Nanoplastics rewire freshwater food webs, *Commun. Earth Environ.*, 2024, **5**, 486.
- 4 J. Gigault, H. El Hadri, B. Nguyen, B. Grassl, L. Roweczyk, N. Tufenkji, S. Y. Feng and M. Wiesner, Nanoplastics are neither microplastics nor engineered nanoparticles, *Nat. Nanotechnol.*, 2021, **16**, 501–507.
- 5 N. B. Hartmann, T. Hüffer, R. C. Thompson, M. Hassellöv, A. Verschoor, A. E. Dugaard, S. Rist, T. Karlsson, N. Brennholt, M. Cole, M. P. Herrling, M. C. Hess, N. P. Ivleva, A. L. Lusher and M. Wagner, Are We Speaking the Same Language? Recommendations for a Definition and Categorization Framework for Plastic Debris, *Environ. Sci. Technol.*, 2019, **53**, 1039–1047.
- 6 A. Ter Halle, L. Jeanneau, M. Martignac, E. Jarde, B. Pedrono, L. Brach and J. Gigault, Nanoplastic in the North Atlantic Subtropical Gyre, *Environ. Sci. Technol.*, 2017, **51**, 13689–13697.
- 7 D. Materic, M. Peacock, J. Dean, M. Futter, T. Maximov, F. Moldan, T. Röckmann and R. Holzinger, Presence of nanoplastics in rural and remote surface waters, *Environ. Res. Lett.*, 2022, **17**, 054036.
- 8 S. Fraissinet, G. E. De Benedetto, C. Malitesta, R. Holzinger and D. Materic, Microplastics and nanoplastics size distribution in farmed mussel tissues, *Commun. Earth Environ.*, 2024, **5**, 128.
- 9 E. Sanfins, C. Augustsson, B. Dahlbäck, S. Linse and T. Cedervall, Size-Dependent Effects of Nanoparticles on Enzymes in the Blood Coagulation Cascade, *Nano Lett.*, 2014, **14**, 4736–4744.
- 10 Statista, *The life cycle of plastics - Statista overview report on the global impact of plastics throughout production, use, and disposal*, <https://www.statista.com/study/83215/the-life-cycle-of-plastics/>.
- 11 A. Wahl, C. Le Juge, M. Davranche, H. El Hadri, B. Grassl, S. Reynaud and J. Gigault, Nanoplastic occurrence in a soil amended with plastic debris, *Chemosphere*, 2021, **262**, 127784.
- 12 S. Lambert and M. Wagner, Characterisation of nanoplastics during the degradation of polystyrene, *Chemosphere*, 2016, **145**, 265–268.
- 13 L. M. Hernandez, J. Grant, P. S. Fard, J. M. Farner and N. Tufenkji, Analysis of ultraviolet and thermal degradations of four common microplastics and evidence of nanoparticle release, *J. Hazard. Mater. Lett.*, 2023, **4**, 100078.
- 14 F. G. Zha, J. M. Dai, Y. X. Han, P. Liu, M. J. Wang, H. Y. Liu and X. T. Guo, Release of millions of micro(nano)plastic fragments from photooxidation of disposable plastic boxes, *Sci. Total Environ.*, 2023, **858**, 160044.
- 15 Z. Y. Liu, Y. J. Zhu, S. S. Lv, Y. X. Shi, S. F. Dong, D. Yan, X. S. Zhu, R. Peng, A. A. Keller and Y. X. Huang, Quantifying the Dynamics of Polystyrene Microplastics UV-Aging Process, *Environ. Sci. Technol. Lett.*, 2022, **9**, 50–56.
- 16 H. Tong, X. Zhong, Z. Duan, X. Yi, F. Cheng, W. Xu and X. Yang, Micro- and nanoplastics released from biodegradable and conventional plastics during degradation: Formation, aging factors, and toxicity, *Sci. Total Environ.*, 2022, **833**, 155275.
- 17 M. T. Ekvall, M. Lundqvist, E. Kelpsiene, E. Sileikis, S. B. Gunnarsson and T. Cedervall, Nanoplastics formed during the mechanical breakdown of daily-use polystyrene products, *Nanoscale Adv.*, 2019, **1**, 1055–1061.
- 18 K. Mattsson, F. Björkroth, T. Karlsson and M. Hassellöv, Nanofragmentation of Expanded Polystyrene Under Simulated Environmental Weathering (Thermooxidative Degradation and Hydrodynamic Turbulence), *Front. Mar. Sci.*, 2021, **7**, 578178.
- 19 B. G. Kwon, K. Koizumi, S. Y. Chung, Y. Kodera, J. O. Kim and K. Saïdo, Global styrene oligomers monitoring as new chemical contamination from polystyrene plastic marine pollution, *J. Hazard. Mater.*, 2015, **300**, 359–367.



- 20 B. G. Kwon, K. Amamiya, H. Sato, S. Y. Chung, Y. Kodera, S. K. Kim, E. J. Lee and K. Saido, Monitoring of styrene oligomers as indicators of polystyrene plastic pollution in the North-West Pacific Ocean, *Chemosphere*, 2017, **180**, 500–505.
- 21 C. P. Ward, C. J. Armstrong, A. N. Walsh, J. H. Jackson and C. M. Reddy, Sunlight Converts Polystyrene to Carbon Dioxide and Dissolved Organic Carbon, *Environ. Sci. Technol. Lett.*, 2019, **6**, 669–674.
- 22 E. Yousif and R. Haddad, Photodegradation and photostabilization of polymers, especially polystyrene: review, *Springerplus*, 2013, **2**, 398.
- 23 A. L. Andradý, P. W. Barnes, J. F. Bornman, T. Gouin, S. Madronich, C. C. White, R. G. Zepp and M. A. K. Jansen, Oxidation and fragmentation of plastics in a changing environment; from UV-radiation to biological degradation, *Sci. Total Environ.*, 2022, **851**, 158022.
- 24 G. Balakrishnan, F. Lagarde, C. Chassenieux, A. Martel, E. Deniau and T. Nicolai, Fate of polystyrene and polyethylene nanoplastics exposed to UV in water, *Environ. Sci.: Nano*, 2023, **10**, 2448–2458.
- 25 X. Y. Wu, X. Chen, R. F. Jiang, J. You and G. F. Ouyang, New insights into the photo-degraded polystyrene microplastic: Effect on the release of volatile organic compounds, *J. Hazard. Mater.*, 2022, **431**, 128523.
- 26 N. M. Ainali, D. N. Bikiaris and D. A. Lambropoulou, Aging effects on low- and high-density polyethylene, polypropylene and polystyrene under UV irradiation: An insight into decomposition mechanism by Py-GC/MS for microplastic analysis, *J. Anal. Appl. Pyrolysis*, 2021, **158**, 105207.
- 27 W. J. Kowalski, *Ultraviolet germicidal irradiation handbook*, 2009.
- 28 S. Peng, L. P. Li, D. B. Wei, M. Chen, F. P. Wang, Y. Gui, X. Y. Zhao and Y. G. Du, Releasing characteristics of toxic chemicals from polystyrene microplastics in the aqueous environment during photoaging process, *Water Res.*, 2024, **258**, 121768.
- 29 L. L. Tian, Q. Q. Chen, W. Jiang, L. H. Wang, H. X. Xie, N. Kalogerakis, Y. N. Ma and R. Ji, A carbon-14 radiotracer-based study on the phototransformation of polystyrene nanoplastics in water versus in air, *Environ. Sci.: Nano*, 2019, **6**, 2907–2917.
- 30 X. R. Qiu, S. R. Ma, J. X. Zhang, L. C. Fang, L. Y. Zhu and X. T. Guo, Dissolved Organic Matter Promotes the Aging Process of Polystyrene Microplastics under Dark and Ultraviolet Light Conditions: The Crucial Role of Reactive Oxygen Species, *Environ. Sci. Technol.*, 2022, **56**, 10149–10160.
- 31 F. Cheng, T. Zhang, Y. Liu, Y. Zhang and J. Qu, Non-Negligible Effects of UV Irradiation on Transformation and Environmental Risks of Microplastics in the Water Environment, *J. Xenobiot.*, 2021, **12**, 1–12.
- 32 K. Mattsson, E. V. Johnson, A. Malmendal, S. Linse, L. A. Hansson and T. Cedervall, Brain damage and behavioural disorders in fish induced by plastic nanoparticles delivered through the food chain, *Sci. Rep.*, 2017, **7**, 11452.
- 33 Z. Meng, R. Recoura-Massaquant, A. Chaumot, S. Stoll and W. Liu, Acute toxicity of nanoplastics on *Daphnia* and *Gammarus* neonates: Effects of surface charge, heteroaggregation, and water properties, *Sci. Total Environ.*, 2023, **854**, 158763.
- 34 A. Pochelon, S. Stoll and V. I. Slaveykova, Polystyrene Nanoplastic Behavior and Toxicity on Crustacean *Daphnia magna*: Media Composition, Size, and Surface Charge Effects, *Environments*, 2021, **8**, 101.
- 35 O. Pikuda, E. Roubeau Dumont, Q. Chen, J.-R. Macairan, S. A. Robinson, D. Berk and N. Tufenkji, Toxicity of microplastics and nanoplastics to *Daphnia magna*: Current status, knowledge gaps and future directions, *TrAC, Trends Anal. Chem.*, 2023, **167**, 117208.
- 36 OECD, *Test No. 202: Daphnia sp. Acute Immobilisation Test*, 2004.
- 37 NORMAN Network, R. Aalizadeh, N. Alygizakis, E. Schymanski, J. Solobodnik, S. Fischer, L. Cirka and H. Mohammed Taha, SO|SUSDAT|Merged NORMAN Suspect List: SusDat (NORMAN-SLE-SO.0.5.1), 2024, DOI: [10.5281/zenodo.2664077](https://doi.org/10.5281/zenodo.2664077).
- 38 S. Bhattacharjee, DLS and zeta potential - What they are and what they are not?, *J. Controlled Release*, 2016, **235**, 337–351.
- 39 J. Almond, P. Sugumaar, M. N. Wenzel, G. Hill and C. Wallis, Determination of the carbonyl index of polyethylene and polypropylene using specified area under band methodology with ATR-FTIR spectroscopy, *e-Polym.*, 2020, **20**, 369–381.
- 40 C. Romera-Castillo, M. Pinto, T. M. Langer, X. A. Alvarez-Salgado and G. J. Herndl, Dissolved organic carbon leaching from plastics stimulates microbial activity in the ocean, *Nat. Commun.*, 2018, **9**, 1430.
- 41 E. Kelpsiene, I. Brandts, K. Bernfur, M. T. Ekvall, M. Lundqvist, M. Teles and T. Cedervall, Protein binding on acutely toxic and non-toxic polystyrene nanoparticles during filtration by *Daphnia magna*, *Environ. Sci.: Nano*, 2022, **9**, 2500–2509.
- 42 W. Liu, X. Wang, X. Zhou, H. Duan, P. Zhao and W. Liu, Quantitative structure-activity relationship between the toxicity of amine surfactant and its molecular structure, *Sci. Total Environ.*, 2020, **702**, 134593.
- 43 N. Phasukarratchai, Effects and applications of surfactants on the release, removal, fate, and transport of microplastics in aquatic ecosystem: a review, *Environ. Sci. Pollut. Res.*, 2023, **30**, 121393–121419.

